CENPK Interacts with SOX6 to Promote Cervical Cancer Stemness and Chemoresistance Through Wnt and P53 Signaling

Xian Lin
Fujian Provincial Cancer Hospital
Feng Wang
Chinese People's Armed Police Force Academy: Chinese People's Police University
Jing Liu
Fujian Provincial Cancer Hospital
Yibin Lin
Fujian Provincial Cancer Hospital
Li Li
Fujian Provincial Cancer Hospital
Zirong Li
Fujian Provincial Cancer Hospital
Junping Pan
Fujian Provincial Cancer Hospital
Yanwen Song
Fujian Provincial Cancer Hospital
Chuanben Chen
Fujian Provincial Cancer Hospital
Qin Xu (xuqinfj@163.com)
Fujian Provincial Cancer Hospital

Research

Keywords: CENPK, SOX6, Stemness, Chemoresistance, Cervical cancer

Posted Date: May 7th, 2021

DOI: https://doi.org/10.21203/rs.3.rs-407627/v1

Abstract

Background

Stemness and chemoresistance contribute to cervical cancer recurrence and metastasis. It is meaningful to develop alternative targets for eliminating cancer stem cells (CSCs) properties, suppressing metastasis, and alleviating chemoresistance in cervical cancer. This study clarifies the role of CENPK in cervical cancer stemness and chemoresistance and its clinical significance in cancer progression.

Methods

Human cervical cancer cell lines, xenografts, and clinical samples were used for expression and functional analysis. CENPK expression in cervical cancer was analyzed by bioinformatics based on a microarray and TCGA database and immunohistochemistry based on 119 paraffin-embedded cervical cancer specimens and 35 paraffin-embedded adjacent normal tissues in a tissue chip.

Results

CENPK served as an oncogene by promoting CSCs properties, DNA damage repair, epithelial-mesenchymal transition and DNA replication, thus inducing cisplatin/carboplatin resistance, cell metastasis and proliferation in cervical cancer. Intriguingly, targeting CENPK markedly prolonged the survival time of cervical cancer-bearing mice, and improved chemotherapy sensitivity of cervical cancer cells *in vivo*. CENPK also interacted with tumor suppressor gene SOX6 to activate Wnt signaling and inactivate p53 signaling. CENPK modulated expression of key regulators in CSCs properties, DNA damage repair, epithelial-mesenchymal transition and DNA replication by disrupting SOX6-β-catenin interaction, promoting β-catenin expression and nuclear translocation, and facilitating SOX6-mediated p53 ubiquitination and nuclear export, thus stimulating cervical cancer stemness, chemoresistance, metastasis and proliferation by. Interestingly, the RAD21/SMC3 complex, downstream targets of β-catenin, enhanced CENPK transcription to form a positive regulatory circuit through Wnt signaling. Facilitation of Wnt signaling by iRhom2 further activated the CENPK/SOX6-β-catenin-RAD21/SMC3 loop and conferred cervical cancer progression, suggesting a Wnt-p53 pathway crosstalk. Importantly, CENPK was upregulated in cervical cancer, correlated with cancer recurrence, and independently predicted poor patient prognosis.

Conclusions

This work identifies CENPK as a prognostic indicator and highlights targeting of CENPK as a novel strategy in the treatment of cervical cancer.

Background

Cervical cancer is the fourth most common cancer in women[1]. According to the latest data, cervical cancer is still the second leading cause of cancer-related death rates among women aged 20 to 39 years[2]. Stemness, chemoresistance, and metastasis of cervical cancer are responsible for treatment failure[3], leading to poor patient prognosis. Therefore, it is meaningful to develop alternative targets for eliminating cancer stem cells (CSCs) properties, suppressing metastasis, and improving the sensitivity to chemotherapy in cervical cancer.

The CENPK gene is located on human chromosome 5, and its encoding protein is composed of 269 amino acids with a molecular weight of 31kD. CENPK acts cooperatively with CENPA and other centromere components to exert its biological effects, which is important for proper mitochondrial function and the mitotic process[4]. CENPK is upregulated in ovarian cancer, breast cancer, hepatocellular carcinoma, bladder cancer, and glioma, and may be related to the malignant progression of tumors[5–9]. However, the relationship between CENPK and cervical cancer development has not been determined, and the underlying mechanism of CENPK in cancer progression is yet to be elucidated.

iRhom2 is a catalytically inactive member of the Rhomboid family and is involved in regulating the activity of multiple signaling pathways in cancers, including the Notch1[10], EGFR[11], and TNF signaling pathways[12]. In addition, iRhom2 functions as an important interactor with metalloproteinase ADAM17 transport factor, which regulates Wnt/β-catenin signaling[13] and modulates the stimulation and substrate selectivity of ADAM17[14]. Our previous study showed that iRhom2 potentiates Wnt signaling activity to regulate the cell cycle, DNA replication, and proliferation of cervical cancer development[15]. However, the biological role of iRhom2 in modulating cervical cancer stemness, chemoresistance, and metastasis, and the signaling pathways with abnormal regulation involved in iRhom2-mediated development of cervical cancer are not fully understood.

Here, we describe a novel CENPK/SOX6-β-catenin-RAD21/SMC3 feedback circuit regulated by iRhom2. The positive regulatory loop promoted cervical cancer stemness, chemoresistance, metastasis, and proliferation. The mechanisms by which CENPK enhanced cervical cancer progression via Wnt/β-catenin and p53 signaling were delineated in detail using cervical cancer cell lines, xenografts, and clinical samples. Targeting CENPK is suggested as an alternative approach for alleviating the CSCs properties and the resistance to platinum chemotherapy in cervical cancer.

Methods

Cell cultures

HeLa and SiHa cell lines were obtained from the Chinese Academy of Sciences Cell Bank (Shanghai, China) and cultured in Dulbecco's modified Eagle's medium supplemented with 10% fetal bovine serum (Biowest, France). Cervical cancer cells were grown at 37°C with 5% CO_2 and 95% room air.

Cell transfections

Lentiviral particles harboring shRNA targeting CENPK (sh-CENPK) and negative control shRNA (sh-NC) were designed and constructed by GeneChem Corporation (Shanghai, China). Lentivirus particles were transfected into cervical cancer cells using polybrene reagent (GeneChem, Inc.). Plasmids (ov-β-catenin, ov-CENPK) were designed and constructed by Vigene Biosciences Corporation (Shandong, China). siRNAs (si-iRhom2, si-CENPK, si-SOX6, si-p53, si-RAD21, si-SMC3) were obtained from RiboBio Corporation (Guangzhou, China) (shown in Additional file 6 Table S1). Following the manufacturer's protocol, plasmids and siRNAs were transduced into cervical cancer cells using Lipofectamine TM 2000 (Invitrogen Corporation, Shanghai, China). Forty-eight to seventy-two hours after transfection, cells were subjected to further experimentation.

Tumorsphere formation assay

The protocol of tumorsphere formation assay was in line with a previous method[16]. Briefly, cervical cancer cells (5,000/well) were seeded on 6-well ultra-low-attachment plates (Corning, Inc., NY, USA) and cultured in serum-free DMEM/F12 with 2% B27, 20 ng/ml EGF, and 20 ng/ml FGF. Fresh medium was replaced every 2 days. The tumorspheres were recorded and counted on day 14 post-seeding, and the number and size of tumorspheres were analyzed after passaging for three generations.

MTT assay

The MTT assay was used to measure cell proliferation. Cervical cancer cells (1,000 cells/well) were seeded in 96-well plates. At the indicated time, MTT (5 mg/ml; Sigma-Aldrich Corporation, MO, USA) was added to each well. After 4 h of incubation, dimethyl sulfoxide (Sigma-Aldrich Corporation, MO, USA) was added to each well. The absorbance value (OD) of each well was detected at 490 nm.

Colony-formation assay

For the measurement of cell proliferation, cervical cancer cells were plated at a density of 100 cells per well. After 10 days of culture, colonies were fixed with methanol and stained with a hematoxylin solution. The number of colonies (≥ 50 cells) was counted under a microscope. For measurement of cell chemoresistance, transfected cervical cancer cells were treated with cisplatin or carboplatin for 6 h at the indicated concentrations before seeding at a density of 500 cells per well. After 10 days of incubation, colonies were fixed, stained, and photographed for analysis.

Transwell assays

Transwell assays were applied to evaluate the migration and invasion capacity of cervical cancer cells. Cells suspension were added to the upper chamber of Transwell coated with (for invasion assay) or without (for migration) Matrigel purchased from BD corporation, and the lower chambers of Transwell were filled with Dulbecco's modified Eagle's medium containing 10% FBS. The migrated and invaded cells were fixed, stained, and photographed under microscopy.

EdU incorporation assays

Following the manufacturer's protocol, EdU incorporation was conducted using the Apollo567 *In Vitro* Imaging Kit (RiboBio Corporation, Guangzhou, China). After 2 h treatment with EdU (10 μM), cervical cancer cells were fixed with 4% paraformaldehyde, permeabilized with 0.3% Triton X-100, and co-stained with Apollo fluorescent dyes and DAPI (5μg/ml). The EdU-positive cells were photographed and counted under a microscope.

Immunofluorescence

Cervical cancer cells were seeded and grew on coverslips. After incubation, the cells were subjected to fixation with 4% paraformaldehyde, permeabilization with 0.2% Triton X-100, and incubation with antibodies (shown in Additional file 7 Table S2). The cells were then co-stained with DAPI (0.2 mg/ml) and observed under a fluorescence confocal microscope.

RT-PCR and QPCR

Total RNA was extracted from cervical cancer cells or xenografts using TRIzol (Invitrogen Corporation, Shanghai, China), and cDNA was generated using a reverse transcription reagent kit (TaKaRa Corporation, Dalian, China). Then, the synthesized cDNA was used as a template for RT-PCR and QPCR with specific primers (shown in Additional file 8 Table S3) on Bio-Rad T100 and Bio-Rad CFX 96, respectively. β-actin was used as a control. For RT-PCR, the images were visualized by Bio-Rad GelDoc XR+. For QPCR, the relative mRNA expression was quantified using the $2^{-\Delta\Delta Ct}$ method.

Western blot analysis

Cervical cancer cells were lysed in lysis buffer, and proteins were quantified by the BCA method. After loading, proteins were separated, transferred, and immunoprobed with specific antibodies (shown in Additional file 7 Table S2). Chemiluminescence was used for protein detection, and images were captured using a Bio-Rad ChemiDocTM CRS+ Molecular Imager.

Animal studies

The Institutional Animal Ethical Committee, Experimental Animal Center of Fujian Medical University approved the protocols for animal studies. All experiments conform to all relevant regulatory standards. BALB/c-nu mice (4-5-week-old, female) (n = 5 per group) were subcutaneously injected with 5×10^6 cells/100 μl in the flank. The longest diameter (A) and the shortest diameter (B) of the growing tumors were measured every 3 days with a caliper, and the tumor volume (V) was calculated by the equation $V = (AB^2)/2$. Twenty days after cell injection, the mice were euthanized and tissue was taken for further experimentation. The subcutaneous xenograft mouse model was constructed and used to evaluate tumor formation ability and tumor growth. A series of 5×10^5, 2×10^5, and 5×10^4 cells inoculated subcutaneously into BALB/c-nu mice (4-5-week-old, female) (n = 6 per group), and the tumor-initiating frequency was evaluated.

A pulmonary metastasis model was applied to detect cervical cancer metastatic ability. BALB/c-nu mice (4-5-week-old, female) (n = 5 per group) were injected with 1×10^6 cells/100 μl through the tail vein. Four weeks after injection, the formation of lung metastasis was evaluated under light and fluorescent microscopy.

The subcutaneous xenograft mouse model was also used to determine the chemoresistance of cervical cancer tumors. Cervical cancer cells (5×10^6 cells/100 μl) were inoculated in the flank of the BALB/c-nu mice (4-5-week-old, female) (n = 10 per group). The mice were treated with cisplatin (3 mg/kg, i.p.) once a week for six weeks[17, 18] or carboplatin (30 mg/kg, i.p.) once a week for four weeks[19]. Survival curves were plotted using Kaplan-Meier analyses.

Luciferase reporter assay

The assays of Wnt signaling activity, p53 signaling activity, and the transcriptional activity of RAD21/SMC3 on CENPK were carried out using the luciferase assay system. Cervical cancer cells were co-transfected with TOPflash or FOPflash with pRL (Millipore Corporation, MA, USA) to detect Wnt signaling. Cervical cancer cells were transfected with pGL4 luciferase reporter vector (Promega Corporation, Madison, USA) harboring p53 response element to detect p53 signaling. Cervical cancer cells were transfected with pGL4 luciferase reporter vector (Promega Corporation, Madison, USA) harboring RAD21/SMC3-binding sites in the CENPK promoter region to detect the transcriptional activity of RAD21/SMC3 on CENPK. Forty-eight hours after transfection, cells were collected and subjected to luciferase activity measurement using the Dual-Luciferase Reporter Assay System (Promega Corporation, Madison, USA) on a BioTek luminometer. The relative activity of each reaction was calculated as the ratio of firefly to Renilla luciferase.

Co-immunoprecipitation (Co-IP)

According to the manufacturer's instructions, Co-IP was conducted with a Pierce Co-Immunoprecipitation kit (Thermo Scientific, Shanghai, China). In brief, total proteins were lysed from cervical cancer cells and subjected to concentration quantification. Proteins (5 mg) were then incubated with specific antibodies or IgG, which was applied as a negative control. The enriched proteins were eluted and used for western blot analysis.

Chromatin immunoprecipitation (ChIP)

The ChIP assay was conducted using a ChIP assay kit (Thermo Scientific, Shanghai, China) according to the manufacturer's instructions. Briefly, chromatin from cervical cancer cells was crosslinked, extracted, and clipped with Micrococcal Nuclease to generate DNA fragments. Immunoprecipitation was performed with specific antibodies (shown in Additional file 7 Table S2) or IgG, which served as a negative control. The DNA fragments were eluted, purified, and subjected to PCR and qPCR.

Cycloheximide (CHX) chase assay

Cervical cancer cells were treated with cycloheximide (50 μg/ml) at the indicated time. Subsequently, proteins were collected and quantified using a BCA method. The proteins were further subjected to western blot analysis, and signals were recorded for evaluating the half-life of the proteins.

Cell fractionation assay

The assay was carried out using NE-PER™ Nuclear and Cytoplasmic Extraction Reagents (Thermo Scientific, Shanghai, China). Cervical cancer cells were sequentially treated with ice-cold CER I and the CER II extraction reagent. After centrifugation, the supernatant containing cytoplasmic extract was collected. The pellet was further incubated with NER extraction reagent. After centrifugation, the supernatant containing nuclear extract was retained. The collected proteins were further subjected to western blot analysis.

Patient tissues

One hundred and nineteen paraffin-embedded cervical cancer specimens and 35 paraffin-embedded adjacent normal tissues in a tissue chip (HUteS154Su01) was purchased from Shanghai Outdo Biotech (Shanghai, China). All the patients underwent surgery and had a confirmed pathological diagnosis. Clinical data were extracted from the medical records of the patients. Some clinicopathological characteristics, such as histology grade and Ki67 status, were not available for all patients. Patient consent and ethics approval were obtained from the Ethics Committee of Shanghai Outdo Biotech Corporation.

Immunohistochemistry (IHC)

Paraffin-fixed sections (4 μm) from tissues were deparaffinized, rehydrated, and subjected to antigen retrieval in citrate buffer. After eradicating endogenous peroxidase activity with 3% H_2O_2 and blocking non-specific antigens with goat serum, the sections were incubated with specific antibodies (shown in Additional file 7 Table S2). The signal of the sections was measured using the DAB substrate (Maixin Biotech. Corporation, Fuzhou, China). Staining intensities were evaluated as previously described[15].

Bioinformatics analysis

The mRNA-Seq data of cervical squamous cell carcinoma and endocervical adenocarcinoma (CESC) in The Cancer Genome Atlas (TCGA) database were downloaded and applied for performing differential expression analysis, correlation analysis, gene set enrichment analysis (GSEA), and gene set variation analysis (GSVA) with R software. The median of mRNA expression values was assigned as a cut-off value, and samples were classified into high- and low-expression groups according to the cut-off value.

Statistical analysis

The data are presented as the mean ± SD from at least three independent experiments and analyzed by SPSS 22.0 or RStudio. Statistical significance was detected using the Student's two-tailed t-test for two groups, one-way ANOVA for multiple groups, and a parametric generalized linear model with random effects for the growth curve. The correlations between CENPK expression and clinical parameters were measured using the Chi-square test. The correlations among gene expressions were measured using Spearman's rank correlation test. The Wilcoxon rank-sum test was applied to investigate the difference of CENPK expression between cancers and adjacent normal tissues. Kaplan-Meier survival curves were plotted for survival analysis, and a log-rank test was used to explore the difference. Cox regression models were adopted to identify the relationship between CENPK and the survival time of cervical cancer patients. All statistical tests were two-sided and a P value of < 0.05 was considered statistically significant. $^{*}P < 0.05$, $^{**}P < 0.01$ and $^{***}P < 0.001$.

Results

CENPK is elevated in cervical cancer and is associated with stemness, chemoresistance, DNA damage repair signaling, and DNA replication

Our previous study demonstrated an oncogenic role for iRhom2 in cervical cancer[15], and its microarray data indicated that iRhom2 knockdown induced the downregulation of 124 genes and the upregulation of 33 genes (fold change ≥ 2.0, P ≤ 0.05). Differential and correlation analyses were then conducted in the TCGA CESC dataset and revealed 19 of the 157 genes that were differentially expressed between tumor and normal tissues and were correlated with iRhom2 expression. Since iRhom2 promotes cell cycle progression and DNA replication in our previous study, GSEA was performed to investigate the correlations between the expression of those 19 genes and the cell cycle and DNA replication. Therein, CENPK, TMPO, UNG, and RCC2 were identified as the genes that potentially mediated the pro-proliferative effect of iRhom2 in cervical cancer (Fig. 1a-c and Additional file 1 Fig. S1a). Moreover, CENPK was confirmed to be the most prominent downstream effector of iRhom2 among these four genes (Additional file 1 Fig. S1b).

CENPK was upregulated in pan-cancer tissues compared to the corresponding normal tissues in TCGA (Additional file 1 Fig. S1c). GSEA and GSVA showed that CENPK was involved in regulating the Wnt, DNA damage repair signaling, cell cycle, and DNA replication (Fig. 1d-f). Since DNA damage repair is closely related to platinum drug resistance and radioresistance, we further collected the platinum drug resistance-associated gene set from KEGG websites and constructed the radioresistance-associated gene set based on a previous study[20]. Intriguingly, GSEA showed that CENPK participated in the modulation of platinum drug resistance, which was more prominent than its regulation of radioresistance (Fig. 1g and Additional file 1 Fig. S1d). In addition, the correlation analyses showed a positive association between CENPK and stemness markers, including EPCAM, CD133, SOX2, and OCT4 (Fig. 1h).

Silencing CENPK suppresses cell CSCs properties, chemoresistance, metastasis, and proliferation in cervical cancer

Considering the bioinformatics results, we then focused on the function of CENPK in cell CSCs properties, chemoresistance, and proliferation in cervical cancer. siRNA and lentivirus were used to knock down CNEPK expression in cervical cancer cells (Additional file 2 Fig. S2). Tumorsphere formation assays and immunofluorescence indicated that CENPK knockdown reduced CSCs properties of HeLa and SiHa cells (Fig. 2a and b). Clonogenic assays revealed that inhibition of CENPK impaired the resistance to cisplatin and carboplatin in HeLa and SiHa cells (Fig. 2c). Transwell assays indicated that silencing of CENPK impaired the migration and invasion capacity in HeLa and SiHa cells (Fig. 2d). MTT and colony formation assays also showed that CENPK knockdown inhibited cell growth in HeLa and SiHa cells (Fig. 2e and f). Interestingly, immunofluorescence showed that downregulation of CENPK enhanced DNA damage as indicated by γH2AX expression in cervical cancer cells treated with platinum drugs (Fig. 2g). Consistent with the bioinformatics results, EdU assays suggested that CENPK knockdown suppressed the percentage of S phase and DNA replication in HeLa and SiHa cells (Fig. 2h). In addition, downregulation of CENPK facilitated the expression of DNA damage repair-associated genes p53 and p21, and suppressed the expression of cell stemness, epithelial-mesenchymal transition (EMT), and DNA replication-associated genes c-Myc, Vimentin, CCND1, and c-Jun (Fig. 2i).

These findings were then tested in animal models using stable CENPK-silenced cervical cancer cells. Subcutaneous tumor xenograft mouse models were applied to evaluate the role of CENPK in cervical cancer. Decreased CENPK expression was confirmed in the tumors treated with CENPK shRNA (Fig. 3a). In the animal model, tumors with CENPK downregulation presented a lower tumor formation ability, a less lung metastasis formation, and a slower growth rate than controls (Fig. 3b-f). IHC also showed a lower expression of Ki67 expression in the CENPK-silenced tumor compared to the controls (Fig. 3g). Interestingly, CENPK silencing prolonged the survival time of the mice, and CENPK downregulation synergized with chemotherapeutic treatment to further extend the survival time of the mice (Fig. 3h).

CENPK interacted with SOX6 to activate Wnt signaling and inactivate p53 signaling in cervical cancer

CENPK was shown to modulate Wnt signaling (Fig. 1d). TOP/FOP-flash assays confirmed the facilitation of Wnt signaling by CENPK (Fig. 4a). To explore the specific mechanism by which CENPK exerted its oncogenic role, we used the BioGRID database (https://downloads.thebiogrid.org/BioGRID) and identified a potential interaction between CENPK and SOX6. In addition, previous studies have demonstrated that SOX6 can activate p53 signaling and inactivate Wnt signaling[21], and can suppress cervical cancer progression[22]. Therefore, SOX6 was selected as a candidate protein interacting with CENPK. Co-IP analyses verified the interaction between CENPK and SOX6 (Fig. 4b). Moreover, colocalization of CENPK and SOX6 was detected in HeLa and SiHa cells (Fig. 4c).

SOX6 inhibits the transcription of target genes regulated by β-catenin through interacting with β-catenin and thereby inactivating Wnt signaling[21]. Moreover, TOP/FOP-flash assays verified the inhibition of Wnt signaling by SOX6 (Fig. 4a), implying that the interaction between CENPK and SOX6 might disrupt the interaction between SOX6 and β-catenin. Co-IP analyses indeed demonstrated the interaction between SOX6 and β-catenin and revealed that CENPK could competitively bind to SOX6 to prevent interaction

between SOX6 and β-catenin (Fig. 4d), thereby activating Wnt signaling. Moreover, immunofluorescence analyses suggested an inhibitory impact of CENPK knockdown on β-catenin expression and nuclear translocation (Fig. 4e). However, we detected no effect of CENPK on SOX6 location or expression (Fig. 4e).

SOX6 could increase the stability of p53 protein by transcriptionally suppressing c-Myc transcription, thus activating p53 signaling in HeLa cells[22]. Accordingly, the effect of CENPK on p53 signaling was further investigated. Dual-luciferase assays showed that CENPK knockdown facilitated p53 signaling and that SOX6 silencing abolished that effect (Fig. 4f). Intriguingly, ChIP assays showed that CENPK knockdown facilitated SOX6 binding to the c-Myc transcription regulatory region (Fig. 4g). Furthermore, CHX chase assays, Co-IP analyses, and cell fraction assays all supported a stimulatory role of CENPK knockdown on p53 stability and an inhibitory role of CENPK knockdown on p53 ubiquitination and nuclear export, these effects all being terminated by SOX6 knockdown (Fig. 4h-j).

Collectively, these data suggested SOX6 mediation of CENPK's effect on Wnt and p53 signaling.

CENPK promotes cervical cancer cell CSCs properties, chemoresistance, metastasis, and proliferation through Wnt and p53 signaling

Next, CENPK function mediated by Wnt and p53 signaling in cervical cancer was further investigated. Tumorsphere formation assays, immunofluorescence, clonogenic assays, MTT, and Edu assays showed that β-catenin overexpression partly reversed the inhibitory effect of CENPK knockdown on cell CSCs properties, resistance to cisplatin and carboplatin, migration, invasion, and growth in HeLa and SiHa cells (Fig. 5a-f). Furthermore, p53 knockdown partially eliminated the suppressive impact of CENPK inhibition on stemness, cisplatin and carboplatin resistance, migration, invasion, and proliferation of HeLa and SiHa cells (Fig. 5a-f). In addition, immunofluorescence and western blot showed that the multiple effects of CENPK knockdown on the expression of DNA damage repair, cell stemness, EMT, and DNA replication-associated genes (γH2AX, p53, p21, c-Myc, Vimentin, CCND1, and c-Jun) could be reversed by β-catenin overexpression or p53 knockdown (Fig. 5g and h).

RAD21/SMC3 transcriptionally promotes CENPK expression and forms a positive regulatory circuit through Wnt signaling

To further illustrate how CENPK expression was regulated, we focused on the CENPK transcription process. Firstly, 1558 identified transcription factors were extracted from the Cistrome Data Browser (http://cistrome.org/db/) database (gene set A). Secondly, the top 1000 genes correlated with CENPK expression were identified using the TCGA CESC dataset (gene set B). From the intersection of these two gene sets, a total of 91 transcription factors were identified. Thirdly, the GTRD database (http://gtrd.biouml.org/) was applied to predict the factors that bound to the promoter region of CENPK based on ChIP-seq experiments performed in cervical cancer cells, and 37 transcription factors were identified with this strategy (gene set C). From the intersection of these three gene sets, we identified RAD21, SMC3, and AFF4 as potential factors regulating CENPK transcription (Fig. 6a).

Intriguingly, GSEA indicated that RAD21 and SMC3 (but not AFF4) participated in regulating DNA damage repair, DNA replication, the cell cycle, and p53 and Wnt signaling (Additional file 3 Fig. S3). We thereby focused on whether RAD21 and SMC3 could facilitate CENPK transcription. Subsequent experiments showed that knockdown of RAD21 or SMC3 downregulated CENPK expression in cervical cancer cells (Fig. 6b). Furthermore, ChIP and dual-luciferase assays showed that endogenous RAD21 and SMC3 bound to the CENPK promoter region (RAD21: chr5, 65563165–65563209; SMC3: chr5, 65563168–65563212) as identified by GTRD and the Cistrome database (Fig. 6c-f).

Interestingly, RAD21 and SMC3 were shown to be target genes of β-catenin[23, 24]. Since CENPK could activate Wnt signaling, we proposed that there was a positive feedback between RAD21/SMC3 and CENPK through Wnt signaling. TOP/FOP-flash assays showed that RAD21 or SMC3 knockdown impaired Wnt signaling activity, but this effect was obliterated by overexpressing CENPK (Fig. 6g). ChIP assays also indicated that inhibition of Wnt signaling suppressed the binding of RAD21/SMC3 to the CENPK promoter region (Fig. 6h). Furthermore, dual-luciferase assay assays showed that inhibition of Wnt signaling facilitated p53 signaling (Fig. 6i). Collectively, these results indicate that RAD21/SMC3 and CENPK formed a feedback loop to drive Wnt/β-catenin signaling, and that there was a link between Wnt and p53 signaling.

iRhom2 modulates the RAD21/SMC3-CENPK/SOX6-mediated Wnt and p53 signaling to potentiate cervical cancer stemness, chemoresistance, metastasis, and proliferation

We previously found that iRhom2 downregulated Wnt signaling to inhibit cell cycle progression and DNA replication in cervical cancer[15]. We thereby investigated the relationship between iRhom2 and the CENPK/SOX6-β-catenin-RAD21/SMC3 feedback loop. RT-qPCR and western blot showed that silencing of iRhom2 decreased CENPK expression (Additional file 4 Fig. S4a), and TOP/FOP luciferase reporter assays and dual-luciferase assays suggested that silencing of iRhom2 decreased Wnt signaling activity and elevated p53 signaling activity. However, these effects were reversed by CENPK overexpression (Additional file 4 Fig. S4b and c). Moreover, iRhom2 knockdown inhibited RAD21/SMC3-mediated CENPK transcription, an effect that was abolished by activating Wnt signaling (Additional file 4 Fig. S4d). Functional and mechanistic analyses suggested that iRhom2 knockdown had a suppressive role in cervical cancer stemness, chemoresistance, metastasis, and proliferation that was terminated by overexpressing CENPK (Additional file 4 Fig. S4e-l).

Relationships between CENPK expression and clinicopathological features of cervical cancer patients

To further establish the role of CENPK, immunohistochemistry was conducted in 119 cervical cancer and 35 adjacent normal tissues. The results showed that CENPK was elevated in cervical cancer relative to adjacent normal tissues (Fig. 7a). Moreover, CENPK protein levels were positively associated with Ki67 protein levels (Fig. 7b) and positively correlated with cancer recurrence (Table 1).

Table 1
Correlations between CENPK expression and the clinicopathological features of cervical cancer patients

Characteristics	n	CENPK expression		*P* value
		Low	High	
Age (years)				
≤Median	58	27 (46.6%)	31 (53.4%)	0.427
Median	61	24 (39.3%)	37 (60.7%)	
pT classification				
T1-T2	96	43 (44.8%)	53 (55.2%)	0.384
T3-T4	23	8 (34.8%)	15 (65.2%)	
pN classification				
N0	97	44 (45.4%)	53 (54.6%)	0.247
N1	22	7 (31.8%)	15 (68.2%)	
Distant metastasis				
No	119	51 (42.9%)	68 (57.1%)	
Yes	0	0 (0.0%)	0 (0.0%)	
Recurrence				
No	80	41 (51.2%)	39 (48.8%)	0.008
Yes	39	10 (25.6%)	29 (74.4%)	
Histology grade				
-	27	12 (44.4%)	15 (55.6%)	0.670
	73	29 (39.7%)	44 (60.3%)	
Ki67 status				
Low expression	56	33 (58.9%)	23 (41.1%)	< 0.001
High expression	41	8 (19.5%)	33 (80.5%)	

Survival analysis suggested that cervical cancer patients with high CENPK expression exhibited poor overall survival (Fig. 7c). Since CENPK expression was correlated with cancer recurrence, we further investigated the relationship between CENPK expression and the recurrence-free survival of cervical cancer patients. Survival analysis showed that cervical cancer patients with high CENPK expression had a poor recurrence-free survival (Fig. 7d). Univariate and multivariate COX hazard analyses were performed

to correlated CENPK, clinicopathological features expression, and overall survival and recurrence-free survival of cervical cancer patients. CENPK expression defined by IHC was an independent and unfavorable prognostic factor for the overall survival and recurrence-free survival of cervical cancer patients (Fig. 7e and f). A nomogram showing the role of CENPK, age, and T classification in predicting cancer recurrence of cervical cancer patients is shown in Fig. 8g; even stratified by age or T classification, CENPK expression was still correlated with the overall survival and recurrence-free survival of cervical cancer patients (Additional file 5 Fig. S5a and b). Consistently, the correlation analyses suggested a positive association between RAD21, SMC3, β-catenin, Ki67, and CENPK expression (Additional file 5 Fig. S5c).

Discussion

Stemness, chemoresistance, metastasis, and tumor size are responsible for cancer recurrence and/or the predicted poor prognosis of cervical cancer patients[25, 26]. In the present study, we demonstrated that CENPK augmented Wnt signaling and attenuated p53 signaling, thus affecting the expression of key regulators of DNA damage repair, EMT and DNA replication, and facilitating the stemness, chemoresistance, metastasis, and proliferation of cervical cancer cells. Downregulation of CENPK delayed the progression of cervical cancer *in vitro* and *in vivo*. Importantly, high CENPK expression in cervical cancer was positively correlated with poor overall survival and recurrence-free survival of cervical cancer patients.

Bioinformatics analyses suggested an oncogenic role of CENPK that may be associated with cell proliferation in cancer[6]. In this work, we consistently found that CENPK stimulated cell CSCs properties, chemoresistance, metastasis, and proliferation in cervical cancer. Interestingly, our mechanism research suggested the interaction between CENPK and SOX6. SOX6 plays a role as a tumor suppressor gene in a variety of cancers[27–29], including cervical cancer[30]. Moreover, SOX6 is a Wnt/β-catenin pathway inhibitor and p53 pathway activator[31, 32]. Here, we demonstrated that CENPK interacted with SOX6 to impair the interaction between SOX6 and β-catenin and SOX6 suppression of c-Myc transcription, thus activating the Wnt pathway and inactivating the p53 pathway. In addition, CENPK's positive regulation of β-catenin expression and nuclear translocation could contribute to the activation of Wnt signaling, which was consistent with previous reports[33, 34]. Nucleotide excision repair is the principal DNA damage repair mechanism in cancer cells with platinum treatment[35], and p53 is a key regulator in nucleotide excision repair that mediates cancer cell resistance to platinum[36]. Wnt signaling could also facilitate cancer cell resistance to platinum through other mechanisms, including regulation of cancer stemness, EMT, and DNA damage repair[16, 37]. In addition, both Wnt and p53 signaling participate in regulating cancer cell stemness, metastasis, and proliferation[38, 39]. In our investigation, we further discovered that CSCs properties, DNA damage repair, EMT, and DNA replication contributed to the promotive role of CENPK on cell resistance to cisplatin and carboplatin, metastasis, and proliferation of cervical cancer through Wnt and p53 signaling.

Previous studies demonstrated that RAD21 and SMC3 belong to the cohesin complex that is responsible for DNA repair, DNA replication, transcription, and p53 signaling[40–42]. In cervical cancer, RAD21 upregulates cell proliferation and downregulates p53 signaling[43]. In this study, we found that RAD21 and SMC3 served downstream of Wnt/β-catenin signaling and directly enhanced CENPK transcription. This suggested that CENPK interacted with SOX6 and worked with the RAD21/SMC3 to form a positive feedback circuit, thus facilitating the activation of Wnt/β-catenin signaling and augmenting cervical cancer progression. SOX6 mediated the effect of RAD21/SMC3-enhanced CENPK on cervical cancer progression, demonstrating that our results are in line with the conclusion drawn in a previous study[43]. We previously found that iRhom2 contributed to cervical cancer progression through activation of Wnt signaling[14]. Here, we further demonstrated that iRhom2 potentiated Wnt signaling and thereby promoted cell stemness, chemoresistance, metastasis, and proliferation in cervical cancer. Considering that CENPK was transcriptionally enhanced by the downstream of Wnt/β-catenin, we assumed that iRhom2 might promote CENPK to affect Wnt and p53 signaling. As expected, iRhom2 upregulated CENPK expression and facilitated the activation of the CENPK/SOX6-β-catenin-RAD21/SMC3 feedback loop. Moreover, we also elucidated a link between Wnt and p53 signaling in cervical cancer, further hinting at their synergistic action in promoting cervical cancer progression.

Bioinformatics and immunohistochemical assays confirmed that CENPK functioned as an oncogene enhancing cervical cancer progression and serving as a prognostic indicator for overall survival and recurrence-free survival of cervical cancer patients. GSEA verified that CENPK was involved in regulating Wnt, chemoresistance, DNA damage repair, the cell cycle, and DNA replication signaling in the TCGA database. Importantly, the identification of CENPK as an independent and unfavorable factor in clinical samples further supported the results obtained from cervical cancer cells.

Conclusions

Overall, our present study provides a new positive regulatory circuit consisting of CENPK, SOX6, β-catenin, RAD21, and SMC3 in the modulation of cervical cancer progression. Furthermore, our study elucidated a novel mechanism by which CENPK could interact with SOX6 to induce a separation between SOX6 and β-catenin, promote β-catenin expression and nuclear translocation, and facilitate p53 ubiquitination and nuclear export, thereby upregulating Wnt signaling and downregulating p53 signaling. Finally, the activation of the CENPK/SOX6-β-catenin-RAD21/SMC3 feedback loop was facilitated by the iRhom2 and synergistically stimulated cervical cancer progression through Wnt signaling (Fig. 8). This work delineates the roles of specific signaling pathways in network crosstalk and highlights the biological basis for the clinical use of CENPK both as a prognostic indicator and as a potential target for cervical cancer treatments.

Abbreviations

CESC: Cervical squamous cell carcinoma and endocervical adenocarcinoma

ChIP: Chromatin immunoprecipitation

CHX: Cycloheximide

Co-IP: Co-immunoprecipitation

CSCs: Cancer stem cells

EMT: epithelial-mesenchymal transition

GSEA: Gene set enrichment analysis

GSVA: Gene set variation analysis

IHC: Immunohistochemistry

TCGA: The Cancer Genome Atlas

Declarations

Ethics approval and consent to participate

Patient consent and ethics approval were obtained from the Ethics Committee of Shanghai Outdo Biotech Corporation. The Institutional Animal Ethical Committee, Experimental Animal Center of Fujian Medical University approved the protocols for animal studies.

Consent for publication

Not applicable

Availability of data and materials

The datasets used and/or analysed during the current study are available from the corresponding author on reasonable request.

Competing interests

The authors declare that they have no competing interests.

Funding

This study was supported by Joint Funds for the Innovation of Science and Technology Program of Fujian Province, China, No. 2018Y9110, and Natural Science Foundation of Fujian Province, China, No. 2020J011126.

Authors' contributions

Q. X. and C.C. conceived and designed this study; X.L. Q.X., and F.W. performed the experiments and prepared the manuscript; X.L., F.W., J.L., Y.B.L., L.L, Z.R.L, J.P.P., and Y.W.S conducted the data analyses. All authors read manuscript drafts, contributed edits, and approved the final manuscript.

Acknowledgements

The authors sincerely compliment the staff of the pathology department for completing the project.

References

1. Sung H, Ferlay J, Siegel RL, Laversanne M, Soerjomataram I, Jemal A, et al. Global cancer statistics 2020: GLOBOCAN estimates of incidence and mortality worldwide for 36 cancers in 185 countries. CA Cancer J Clin. 2021. doi:10.3322/caac.21660.
2. Siegel RL, Miller KD, Jemal A. Cancer statistics, 2020. CA Cancer J Clin. 2020;70:7–30.
3. He Y, Xiao M, Fu H, Chen L, Qi L, Liu D, et al. cPLA2α reversibly regulates different subsets of cancer stem cells transformation in cervical cancer. Stem Cells. 2020;38:487–503.
4. Okada M, Cheeseman IM, Hori T, Okawa K, McLeod IX, Yates JR, et al. The CENP-H-I complex is required for the efficient incorporation of newly synthesized CENP-A into centromeres. Nat Cell Biol. 2006;8:446–57.
5. Lee YC, Huang CC, Lin DY, Chang WC, Lee KH. Overexpression of centromere protein K (CENPK) in ovarian cancer is correlated with poor patient survival and associated with predictive and prognostic relevance. PeerJ. 2015;3:e1386.
6. Komatsu M, Yoshimaru T, Matsuo T, Kiyotani K, Miyoshi Y, Tanahashi T, et al. Molecular features of triple negative breast cancer cells by genome-wide gene expression profiling analysis. Int J Oncol. 2013;42:478–506.
7. Wang H, Liu W, Liu L, Wu C, Wu W, Zheng J, et al. Overexpression of centromere protein K (CENP-K) gene in hepatocellular carcinoma promote cell proliferation by activating AKT/TP53 signal pathway. Oncotarget. 2017;8:73994–4005.
8. Liu Y, Xiong S, Liu S, Chen J, Yang H, Liu G, et al. Analysis of Gene Expression in Bladder Cancer: Possible Involvement of Mitosis and Complement and Coagulation Cascades Signaling Pathway. J Comput Biol. 2020;27:987–98.
9. Liu Y, Hu H, Zhang C, Wang H, Zhang W, Wang Z, et al. Co-expression of mitosis-regulating genes contributes to malignant progression and prognosis in oligodendrogliomas. Oncotarget. 2015;6:38257–69.
10. Wang R, Li Y, Tsung A, Huang H, Du Q, Yang M, et al. iNOS promotes CD24(+)CD133(+) liver cancer stem cell phenotype through a TACE/ADAM17-dependent Notch signaling pathway. Proc Natl Acad Sci U S A. 2018;115:E10127–36.
11. Cataisson C, Michalowski AM, Shibuya K, Ryscavage A, Klosterman M, Wright L, et al. MET signaling in keratinocytes activates EGFR and initiates squamous carcinogenesis. Sci Signal. 2016;9:ra62.

12. Maney SK, McIlwain DR, Polz R, Pandyra AA, Sundaram B, Wolff D, et al. Deletions in the cytoplasmic domain of iRhom1 and iRhom2 promote shedding of the TNF receptor by the protease ADAM17. Sci Signal. 2015;8:ra109.
13. Schmidt S, Schumacher N, Schwarz J, Tangermann S, Kenner L, Schlederer M, et al. ADAM17 is required for EGF-R-induced intestinal tumors via IL-6 trans-signaling. J Exp Med. 2018;215:1205–25.
14. Tang B, Li X, Maretzky T, Perez-Aguilar JM, McIlwain D, Xie Y, et al. Substrate-selective protein ectodomain shedding by ADAM17 and iRhom2 depends on their juxtamembrane and transmembrane domains. Faseb j. 2020;34:4956–69.
15. Xu Q, Chen C, Liu B, Lin Y, Zheng P, Zhou D, et al. Association of iRhom1 and iRhom2 expression with prognosis in patients with cervical cancer and possible signaling pathways. Oncol Rep. 2020;43:41–54.
16. Zou Y, Lin X, Bu J, Lin Z, Chen Y, Qiu Y, et al. Timeless-Stimulated miR-5188-FOXO1/β-Catenin-c-Jun Feedback Loop Promotes Stemness via Ubiquitination of β-Catenin in Breast Cancer. Mol Ther. 2020;28:313–27.
17. Zhou F, Yang X, Zhao H, Liu Y, Feng Y, An R, et al. Down-regulation of OGT promotes cisplatin resistance by inducing autophagy in ovarian cancer. Theranostics. 2018;8:5200–12.
18. Segovia-Mendoza M, Jurado R, Mir R, Medina LA, Prado-Garcia H, Garcia-Lopez P. Antihormonal agents as a strategy to improve the effect of chemo-radiation in cervical cancer: in vitro and in vivo study. BMC Cancer. 2015;15:21.
19. Mukherjee A, Chiang CY, Daifotis HA. Adipocyte-Induced FABP4 Expression in Ovarian Cancer Cells Promotes Metastasis and Mediates Carboplatin Resistance. Cancer Res. 2020;80:1748–61.
20. Kitahara O, Katagiri T, Tsunoda T, Harima Y, Nakamura Y. Classification of sensitivity or resistance of cervical cancers to ionizing radiation according to expression profiles of 62 genes selected by cDNA microarray analysis. Neoplasia. 2002;4:295–303.
21. Dong P, Xiong Y, Yu J, Chen L, Tao T, Yi S, et al. Control of PD-L1 expression by miR-140/142/340/383 and oncogenic activation of the OCT4-miR-18a pathway in cervical cancer. Oncogene. 2018;37:5257–68.
22. Wang J, Ding S, Duan Z, Xie Q, Zhang T, Zhang X, et al. Role of p14ARF-HDM2-p53 axis in SOX6-mediated tumor suppression. Oncogene. 2016;35:1692–702.
23. Ghiselli G, Coffee N, Munnery CE, Koratkar R, Siracusa LD. The cohesin SMC3 is a target the for beta-catenin/TCF4 transactivation pathway. J Biol Chem. 2003;278:20259–67.
24. Xu H, Yan Y, Deb S, Rangasamy D, Germann M, Malaterre J, et al. Cohesin Rad21 mediates loss of heterozygosity and is upregulated via Wnt promoting transcriptional dysregulation in gastrointestinal tumors. Cell Rep. 2014;9:1781–97.
25. Xie Q, Liang J, Rao Q, Xie X, Li R, Liu Y, et al. Aldehyde Dehydrogenase 1 Expression Predicts Chemoresistance and Poor Clinical Outcomes in Patients with Locally Advanced Cervical Cancer Treated with Neoadjuvant Chemotherapy Prior to Radical Hysterectomy. Ann Surg Oncol. 2016;23:163–70.

26. Lee SW, Lee SH, Kim J, Kim YS, Yoon MS, Jeong S, et al. Magnetic resonance imaging during definitive chemoradiotherapy can predict tumor recurrence and patient survival in locally advanced cervical cancer: A multi-institutional retrospective analysis of KROG 16 – 01. Gynecol Oncol. 2017;147:334–9.
27. Jiang W, Yuan Q, Jiang Y, Huang L, Chen C, Hu G, et al. Identification of Sox6 as a regulator of pancreatic cancer development. J Cell Mol Med. 2018;22:1864–72.
28. Liang Z, Xu J, Gu C. Novel role of the SRY-related high-mobility-group box D gene in cancer. Semin Cancer Biol. 2020;67:83–90.
29. Lin M, Lei T, Zheng J, Chen S, Du L, Xie H. UBE2S mediates tumor progression via SOX6/β-Catenin signaling in endometrial cancer. Int J Biochem Cell Biol. 2019;109:17–22.
30. Chen Y, Song Y, Mi Y, Jin H, Cao J, Li H, et al. microRNA-499a promotes the progression and chemoresistance of cervical cancer cells by targeting SOX6. Apoptosis. 2020;25:205–16.
31. Chen L, Xie Y, Ma X, Zhang Y, Li X, Zhang F, et al. SOX6 represses tumor growth of clear cell renal cell carcinoma by HMG domain-dependent regulation of Wnt/β-catenin signaling. Mol Carcinog. 2020;59:1159–73.
32. Kurtsdotter I, Topcic D, Karlén A, Singla B, Hagey DW, Bergsland M, et al. SOX5/6/21 Prevent Oncogene-Driven Transformation of Brain Stem Cells. Cancer Res. 2017;77:4985–97.
33. He Y, Davies CM, Harrington BS, Hellmers L, Sheng Y. CDCP1 enhances Wnt signaling in colorectal cancer promoting nuclear localization of β-catenin and E-cadherin. Oncogene. 2020;39:219–33.
34. Lin X, Zuo S, Luo R, Li Y, Yu G, Zou Y, et al. HBX-induced miR-5188 impairs FOXO1 to stimulate β-catenin nuclear translocation and promotes tumor stemness in hepatocellular carcinoma. Theranostics. 2019;9:7583–98.
35. Kong YW, Dreaden EC, Morandell S, Zhou W, Dhara SS. Enhancing chemotherapy response through augmented synthetic lethality by co-targeting nucleotide excision repair and cell-cycle checkpoints. Nat Commun. 2020;11:4124.
36. Bowden NA, Ashton KA, Avery-Kiejda KA, Zhang XD, Hersey P, Scott RJ. Nucleotide excision repair gene expression after Cisplatin treatment in melanoma. Cancer Res. 2010;70:7918–26.
37. Zhong Z, Virshup DM. Wnt Signaling and Drug Resistance in Cancer. Mol Pharmacol. 2020;97:72–89.
38. Yu CS, Chen F, Wang XQ, Cai ZM, Yang MX, Zhong QW, et al. Pin2 telomeric repeat factor 1-interacting telomerase inhibitor 1 (PinX1) inhibits nasopharyngeal cancer cell stemness: implication for cancer progression and therapeutic targeting. J Exp Clin Cancer Res. 2020;39:31.
39. Lin X, Li AM, Li YH, Luo RC, Zou YJ, Liu YY, et al. Silencing MYH9 blocks HBx-induced GSK3β ubiquitination and degradation to inhibit tumor stemness in hepatocellular carcinoma. Signal Transduct Target Ther. 2020;5:13.
40. Yun J, Song SH, Kang JY, Park J, Kim HP, Han SW, et al. Reduced cohesin destabilizes high-level gene amplification by disrupting pre-replication complex bindings in human cancers with chromosomal instability. Nucleic Acids Res. 2016;44:558–72.

41. Zhang N, Kuznetsov SG, Sharan SK, Li K, Rao PH, Pati D. A handcuff model for the cohesin complex. J Cell Biol. 2008;183:1019–31.
42. Ghiselli G. SMC3 knockdown triggers genomic instability and p53-dependent apoptosis in human and zebrafish cells. Mol Cancer. 2006;5:52.
43. Xia L, Wang M, Li H, Tang X, Chen F, Cui J. The effect of aberrant expression and genetic polymorphisms of Rad21 on cervical cancer biology. Cancer Med. 2018;7:3393–405.

Figures

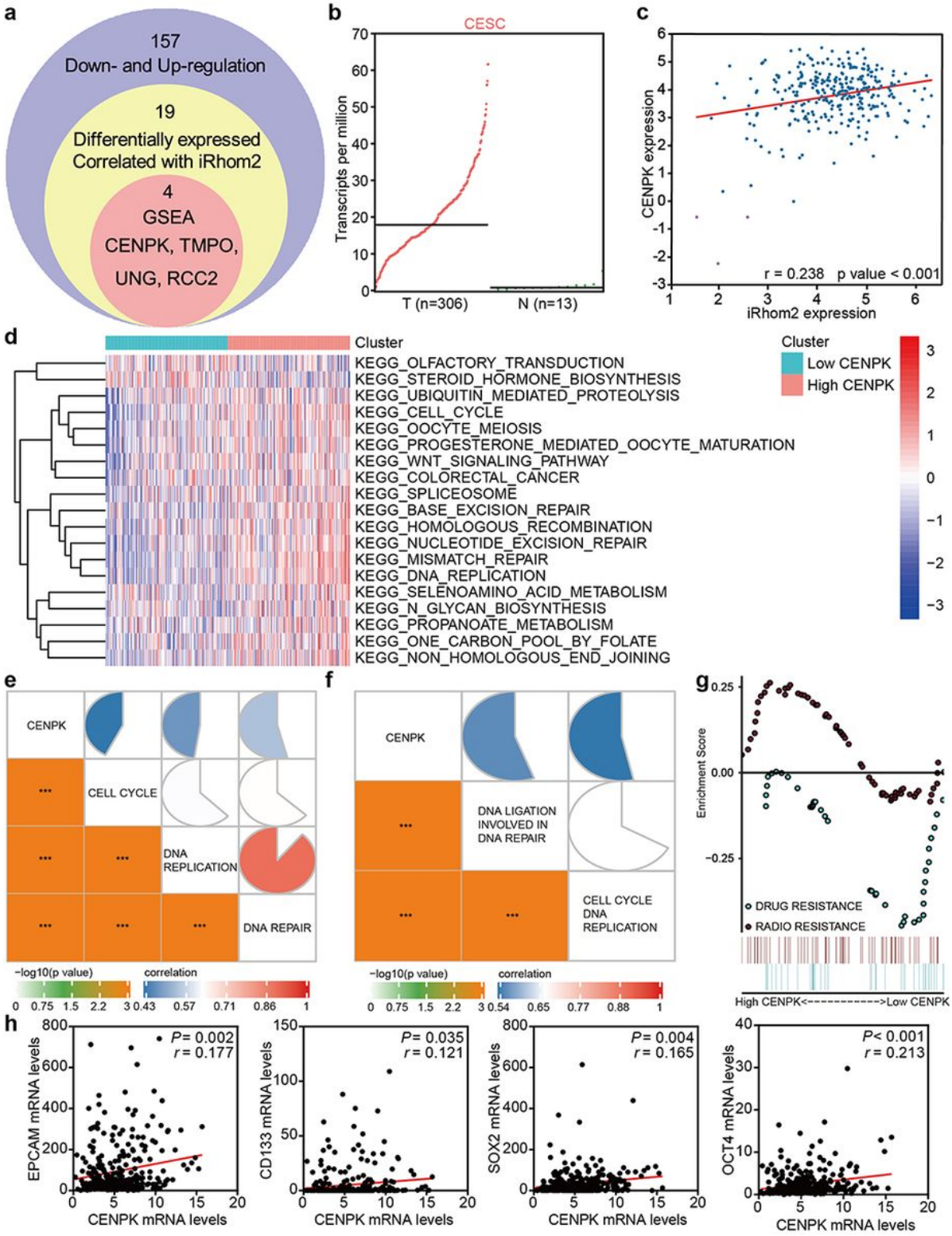

Figure 1

The bioinformatics analyses of iRhom2-regulated CENPK based on the microarray and TCGA data. (a) A Venn diagram analysis for searching the potential downstream effectors of iRhom2. (b) Comparison of CENPK expression between cervical cancer and adjacent normal tissues. (c) The relationship between iRhom2 and CENPK expression. (d) Heatmap of the differential enrichment of the gene sets that participated in regulating the Wnt, cell cycle, DNA replication, and DNA damage repair signaling between

high and low CENPK expression. (e) The relationship between CENPK expression and the cell cycle, DNA replication, and DNA repair determined by GSVA based on KEGG gene sets. (f) The relationship between CENPK expression and the cell cycle, DNA replication, and DNA repair determined by GSVA based on GO function gene sets. (g) GSEA of CENPK showed enrichment of the gene sets that participated in regulating platinum resistance and radioresistance. (h) The relationships among EPCAM, CD133, SOX2, OCT4, and CENPK expression. TCGA: The Cancer Genome Atlas; GSVA: Gene set variation analysis; GSEA: Gene set enrichment analysis.

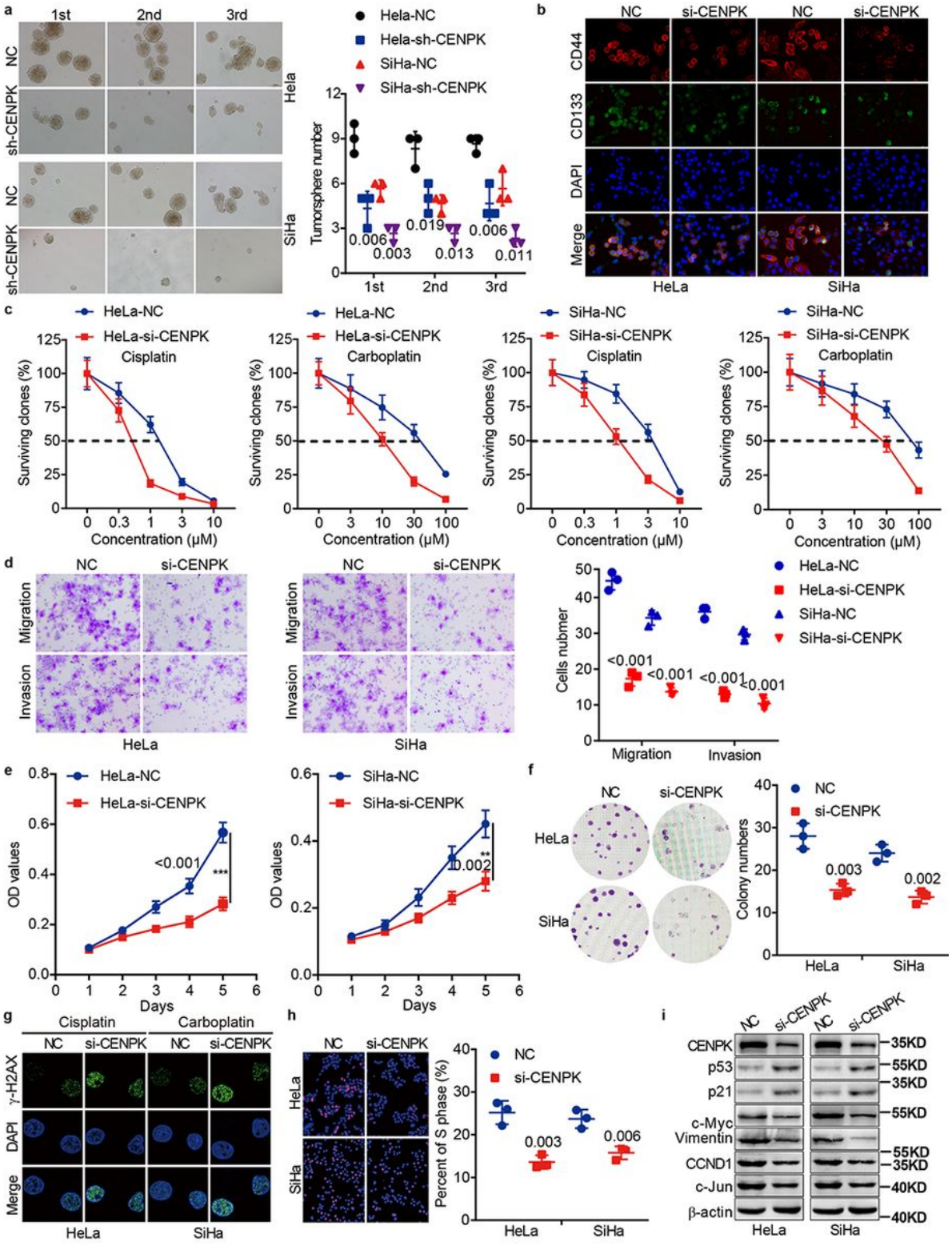

Figure 2

CENPK promotes cervical cancer stemness, chemoresistance, metastasis, and proliferation. Tumorsphere formation assays (a) and immunofluorescence assays (400×) (b) of CENPK-silenced HeLa and SiHa cells and the control cells. (c) Clonogenic assays of CENPK-silenced HeLa and SiHa cells and the control cells treated with cisplatin and carboplatin. Transwell assays (200×) (d), MTT assays (e), and colony-formation assays (f) of CENPK-silenced HeLa and SiHa cells and the control cells. (g) Immunofluorescence to detect the expression of γH2AX in CENPK-silenced HeLa treated with cisplatin, CENPK-silenced SiHa cells treated with carboplatin, and control cells (400×). (h) EdU incorporation assays of CENPK-silenced HeLa and SiHa cells and the control cells (200×). (i) Western blot analysis of CSCs properties, DNA damage repair, epithelial-mesenchymal transition, and DNA replication-associated protein expression in CENPK-silenced HeLa and SiHa cells and control cells. Data are represented as mean ± SD. CSCs: Cancer stem cells.

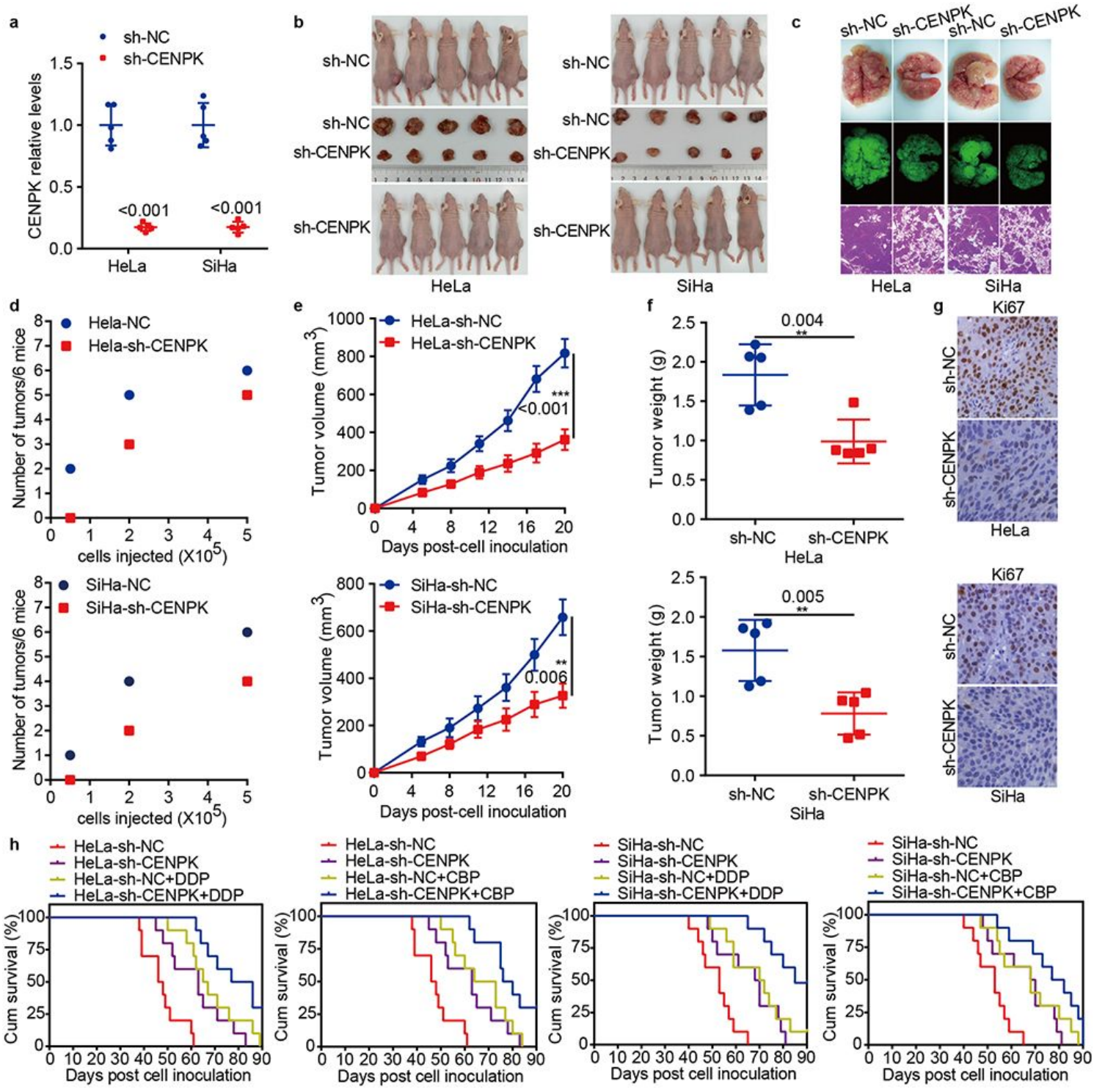

Figure 3

CENPK enhances cervical cancer stemness, chemoresistance, metastasis, and proliferation in vivo. (a) QPCR analyses of CENPK levels in HeLa and SiHa-derived xenografts with CENPK silencing and controls. (b-g) The subcutaneous xenograft mouse model was established to evaluate the effect of CENPK on cervical cancer stemness, metastasis, and proliferation. Tumor formation ability, tumor volume, and tumor weight were calculated and recorded. Xenograft tumors were subjected to detection of Ki67 expression by immunohistochemistry (200×). (h) Survival analyses were performed to compare the

overall survival time of the mice in the CENPK-silenced group, the cisplatin/carboplatin-treated group, the CENPK knockdown plus cisplatin/carboplatin-treated group, and the controls. Data are represented as mean ± SD.

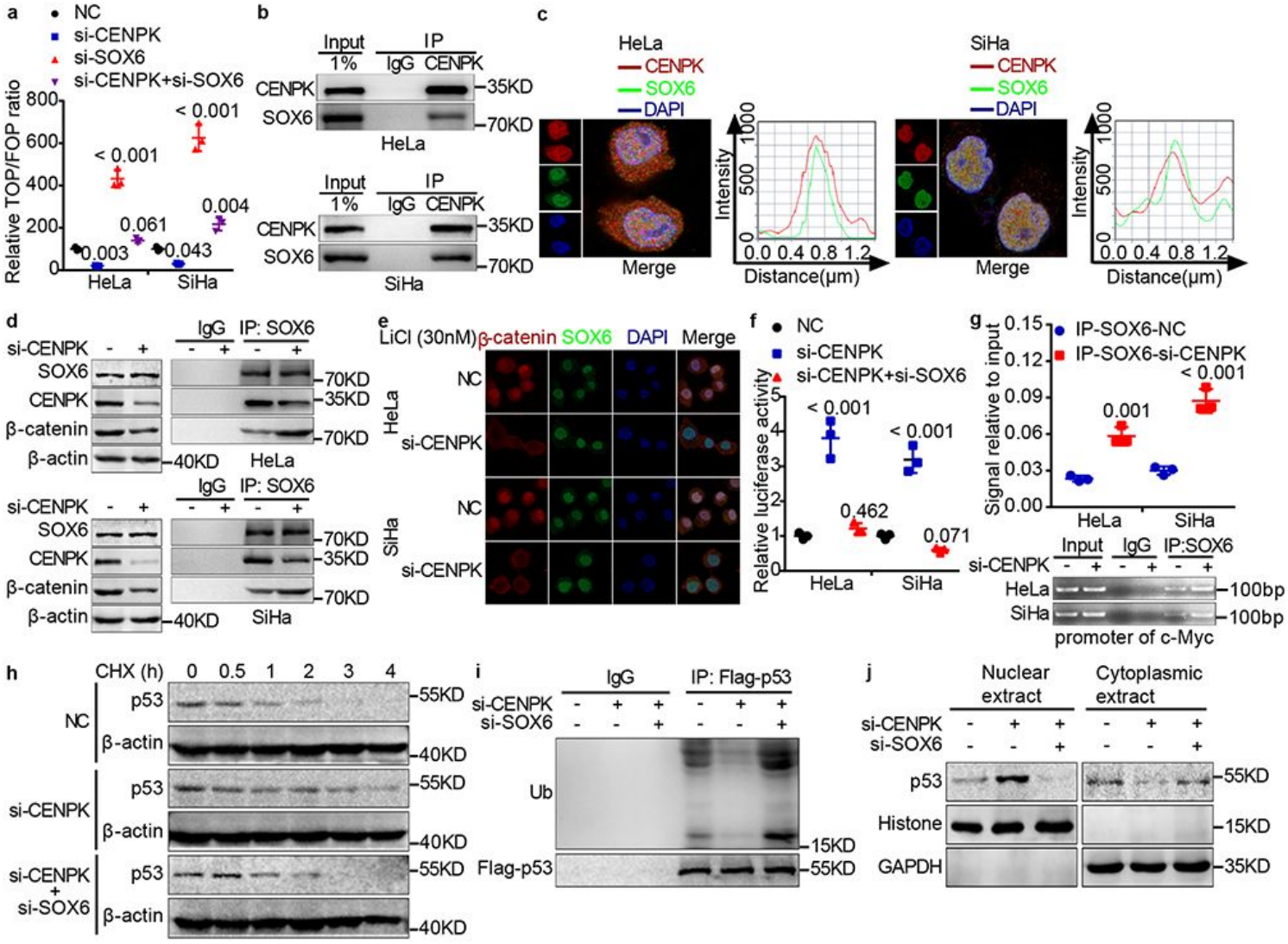

Figure 4

CENPK interacts with SOX6 to activate Wnt signaling and inactivate p53 signaling in cervical cancer. (a) TOP/FOP luciferase reporter assays were conducted to measure the effect of CENPK and SOX6 on Wnt signaling activity. (b) Co-immunoprecipitation analyses were conducted to detect the interaction between CENPK and SOX6. (c) Immunofluorescence co-staining of CENPK and SOX6 was carried out to measure the colocalization of CENPK and SOX6. The red bar represented the colocalization of CENPK and SOX6. (d) Co-immunoprecipitation analyses were conducted to evaluate the effect of CENPK on the interaction between SOX6 and β-catenin. (e) Immunofluorescence co-staining of β-catenin and SOX6 was carried out to investigate the effect of CENPK on the expression and nuclear translocation of β-catenin and SOX6 in HeLa and SiHa cells treated with lithium (400×). (f) Luciferase reporter assays were performed to elucidate the effect of CENPK and SOX6 on p53 signaling activity. (g) Chromatin immunoprecipitation analyses were applied to estimate the impact of CENPK on the binding of SOX6 to the regulatory region

of c-Myc. (h) CHX chasing assays were used to assess the impact of CENPK and SOX6 on p53 stability in HeLa cells. (i) Co-immunoprecipitation analyses were conducted to verify the impact of CENPK and SOX6 on p53 ubiquitination in HeLa cells treated with MG132. (j) Cell fraction assays were performed to validate the impact of CENPK and SOX6 on p53 nuclear export in HeLa cells. Comparison of all groups vs. control group. Data are represented as mean ± SD. CHX: Cycloheximide.

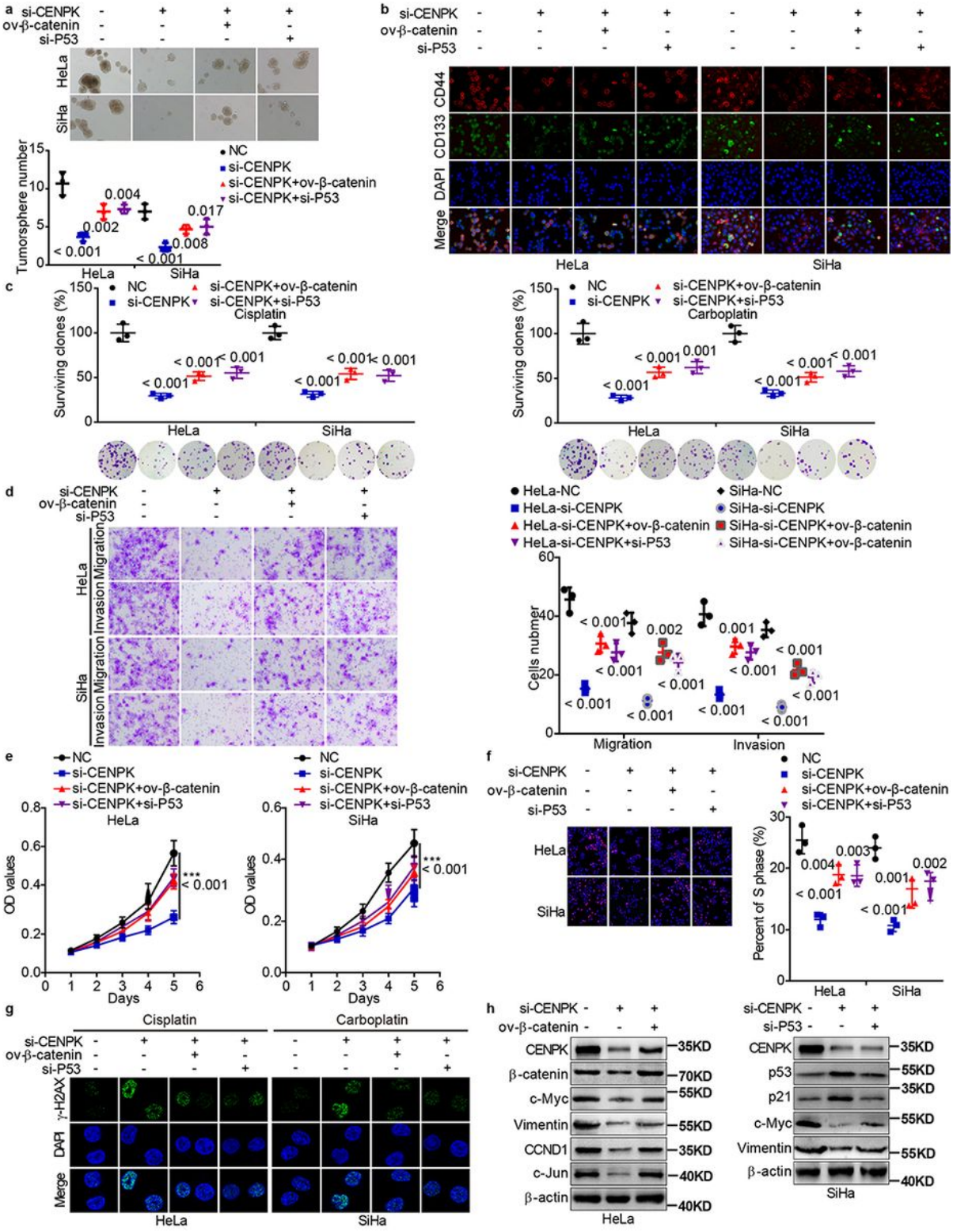

Figure 5

CENPK augments cervical cancer stemness, chemoresistance, metastasis, and proliferation through Wnt and p53 signaling. Tumorsphere formation assays (a) and immunofluorescence assays (400×) (b) of CENPK-silenced HeLa and SiHa cells, CENPK-silenced HeLa and SiHa cells with β-catenin overexpression, CENPK-silenced HeLa and SiHa cells with p53 knockdown, and the control cells. (c) Clonogenic assays were performed to assess the resistance to cisplatin and carboplatin in CENPK-silenced HeLa and SiHa cells, CENPK-silenced HeLa and SiHa cells with β-catenin overexpression, CENPK-silenced HeLa and SiHa cells with p53 knockdown, and the control cells. Transwell assays (200×) (d), MTT assays (e), and EdU incorporation assays (200×) (f) of CENPK-silenced HeLa and SiHa cells, CENPK-silenced HeLa and SiHa cells with β-catenin overexpression, CENPK-silenced HeLa and SiHa cells with p53 knockdown, and the control cells. (g) Immunofluorescence was performed to detect the expression of γH2AX in CENPK-silenced HeLa and SiHa cells, CENPK-silenced HeLa and SiHa cells with β-catenin overexpression, CENPK-silenced HeLa and SiHa cells with p53 knockdown, and the control cells following cisplatin or carboplatin treatment (400×). (h) Western blot analysis of CSCs properties, DNA damage repair, epithelial-mesenchymal transition, and DNA replication-associated proteins expression in CENPK-silenced HeLa and SiHa cells, CENPK-silenced HeLa cells with β-catenin overexpression, CENPK-silenced SiHa cells with p53 knockdown, and the control cells. Comparison of all groups vs. control group. Data are represented as mean ± SD. CSCs: Cancer stem cells.

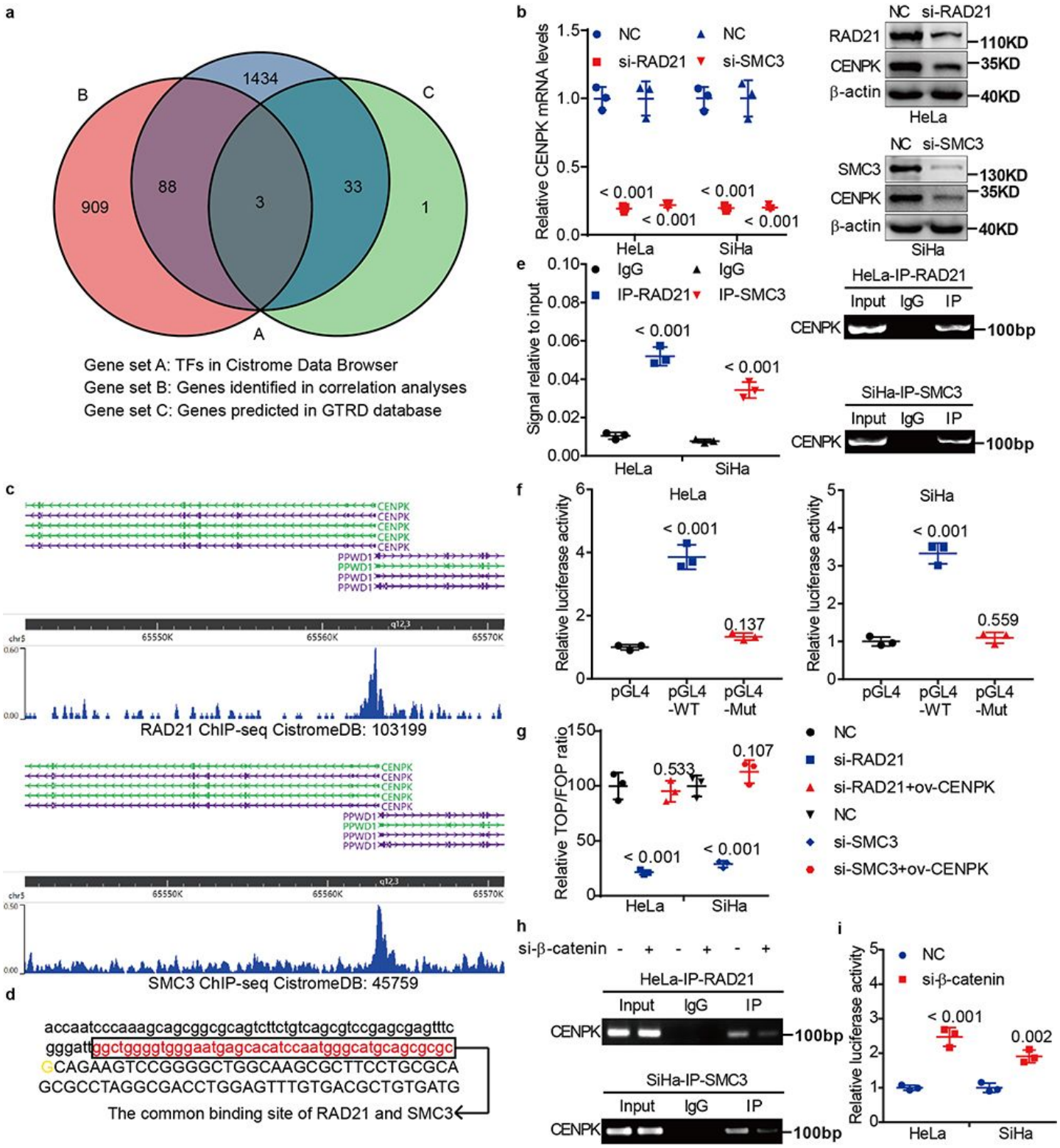

Figure 6

RAD21/SMC3 transcriptionally promotes CENPK expression to shape a positive regulatory circuit. (a) Bioinformatics analyses identified the potential transcription factors that enhanced CENPK transcription. (b) QPCR and western blot analyses were conducted to estimate the effect of RAD21/SMC3 knockdown on CENPK expression. (c) ChIP-seq binding peaks were shown in the Cristome Data Browser database. (d) Bioinformatics analysis was applied to predict RAD21/SMC3-binding site within the promoter of

CENPK. Red: the common binding site of RAD21 and SMC3. Yellow: the transcription start site of CENPK. (e) Chromatin immunoprecipitation analyses were applied to evaluate the interplay between RAD21/SMC3 and CENPK promoter. (f) Luciferase reporter assays were conducted to confirm the binding of RAD21/SMC3 to CENPK promoter. (g) TOP/FOP luciferase reporter assays were performed to measure the effect of RAD21/SMC3 and CENPK on Wnt signaling activity. (h) Chromatin immunoprecipitation analyses were applied for evaluating the effect of Wnt signaling on RAD21/SMC3-mediated CENPK transcription. (i) Luciferase reporter assays were used for confirming the effect of Wnt signaling on p53 signaling activity. Comparison of all groups vs. control group. Data are represented as mean ± SD. ChIP: Chromatin immunoprecipitation.

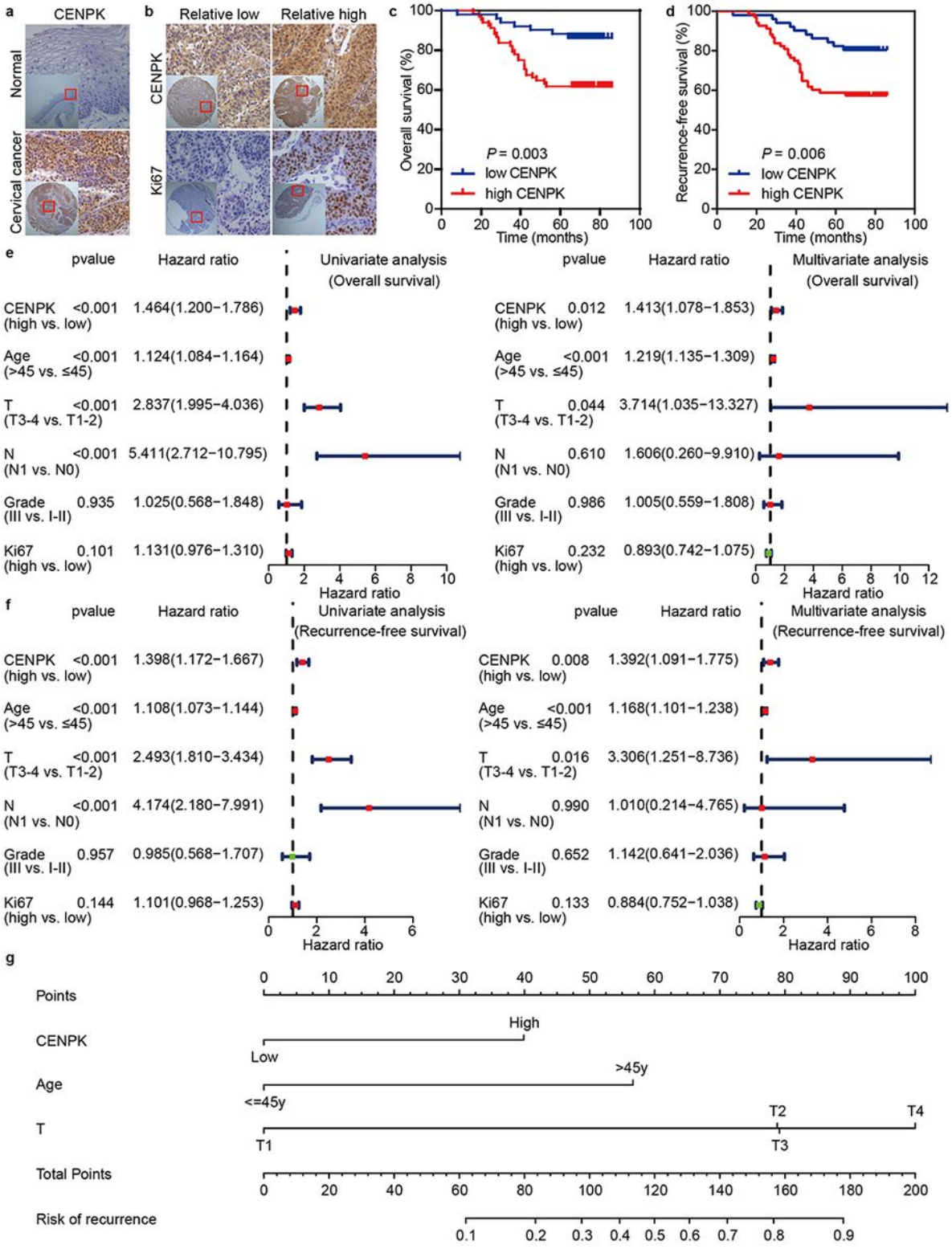

Figure 7

CENPK is upregulated in cervical cancer and confers poor patient prognosis. (a) Representative images showing the differential CENPK expression between cervical cancer and adjacent normal tissues. (b) Representative images showing the relationship between CENPK and Ki67 expression in cervical cancer. (c) Kaplan-Meier survival analysis was conducted to disclose the overall survival of cervical cancer patients according to CENPK expression. (d) Kaplan-Meier survival analysis was conducted to display the

recurrence-free survival of cervical cancer patients according to CENPK expression. (e) Univariate and multivariate analyses were performed to correlate CENPK expression, clinicopathological characteristics, and overall survival of cervical cancer patients. (f) Univariate and multivariate analyses were performed to correlate CENPK expression, clinicopathological characteristics, and recurrence-free survival of cervical cancer patients. (g) Development of a nomogram for predicting cancer recurrence of cervical cancer patients.

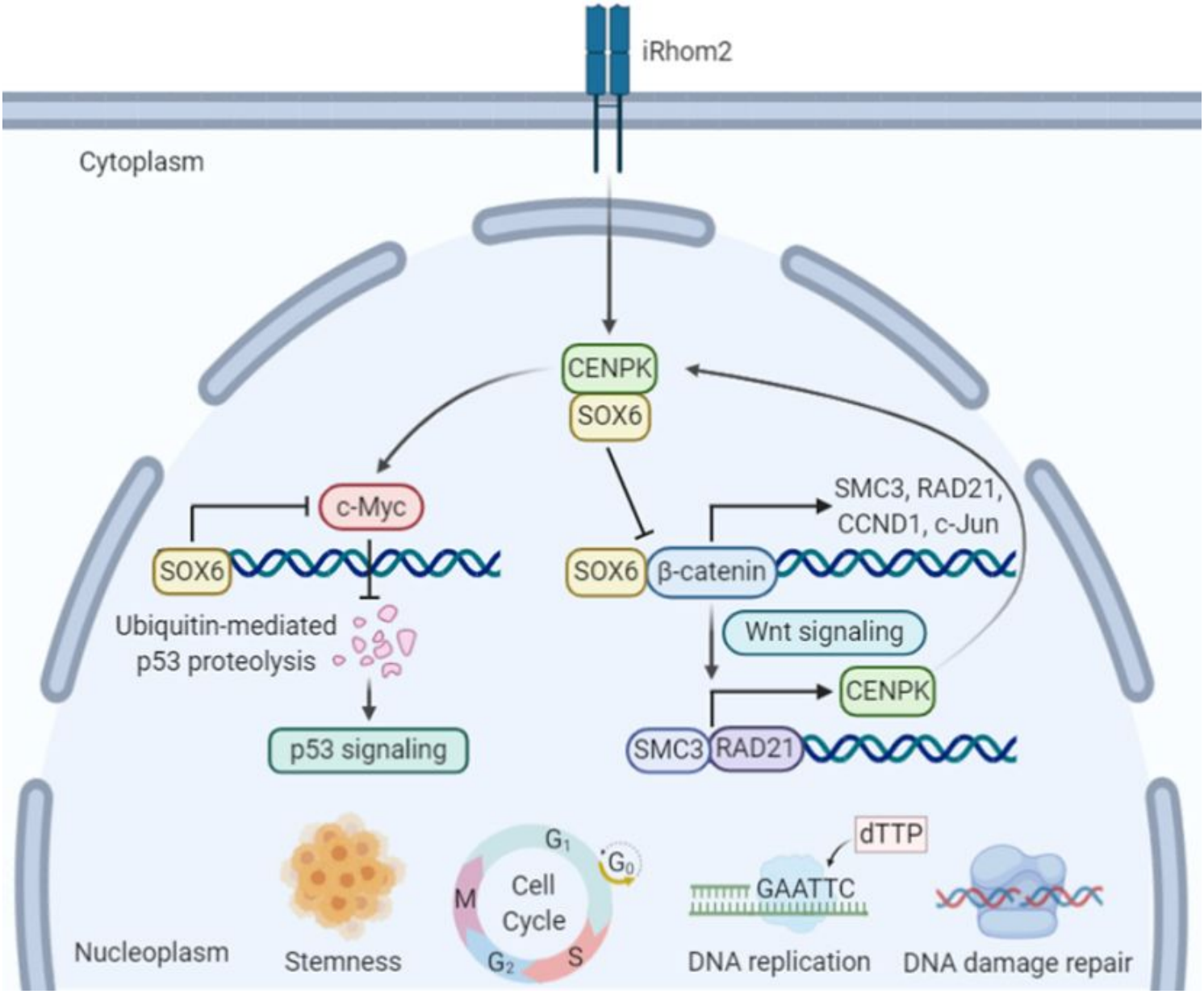

Figure 8

Working model of the CENPK/SOX6-β-catenin-RAD21/SMC3 regulatory loop triggered by iRhom2 in controlling stemness, cell cycle, DNA replication, and DNA repair through Wnt and p53 signaling.

Supplementary Files

This is a list of supplementary files associated with this preprint. Click to download.

- SupplementaryMaterial.doc